Supporting Information

Kastrup et al. 10.1073/pnas.1217972110

SI Text

Local Biocompatibility in the Vessel Wall. The biocompatibility was assessed by histological analysis of the hydrogel coated on the inside of carotid arteries of mice (Fig. 2; Figs. S4 *E–J* and S5; day 4 and 4 mo). This test is the most conclusive test for local biocompatibility in the vasculature. These results showed that the gel alone does not elicit chronic local inflammation in the vasculature. In fact, when combined with an anti-inflammation therapy, the gel actually reduced inflammation. An acute, low-level inflammatory response, typical of implanted biomaterials, was seen after 4 d, which was likely the stimulus for the growth of smooth muscle cells (Fig. S5).

Testing Toxicity in Vitro. The toxicity of alginate-catechol was assessed on cells in vitro using human umbilical vein endothelial cells (HUVECs) and the water-soluble tetrazolium salt (WST-1) proliferation assay (Fig. S1*B*), with the goal of determining whether components released from the gel, such as trace amounts of $NaIO_4$, would be toxic to cells. HUVECs were seeded on the permeable supports of a 96-well transwell plate (3 μm pore size polycarbonate membrane; Corning). Each well was filled with 100 μL of a solution of cells at a concentration of 60,000 cells/mL of growth media and then incubated at 37 °C, 5% CO_2 for 24 h. Into the receiver well of the 96-well transwell plate was added 200 μL of growth media only (positive control), a cell-killing solution of 200 μL H_2O_2 (50 mM in growth media) (negative control), or alginate-catechol with the $NaIO_4$ gelation solution (1, 5, or 10 μL of alginate catechol was allowed to gel in the plate, followed by addition of the growth media). The cells were then incubated in the transwell receiver plate for 24 h before assaying for cell proliferation. The WST-1 assay (Cayman Chemical) provides a method to measure cell proliferation based on the enzymatic cleavage of the tetrazolium salt WST-1 to a water-soluble formazan dye, which can be detected by absorbance at 420–480 nm. The WST-1 reagent was added to each well and incubated according to the supplier protocol and was measured using a microplate reader at 450 nm.

Measuring Body Mass After i.p. Injections. In addition to analyzing local compatibility, biocompatibility was also assessed by injecting alginate-catechol into the peritoneum of mice and measuring the change in body mass over time (Fig. S1 *C* and *D*). Cage-side observations and measuring the body mass for an extended period following a large injection of the material gives an indication of chronic toxicity and provides an indication of overall health and stress of the animal to the material (1). Mice (BALB/c strain; Charles River Laboratories) were injected with 75 μL of saline (control) or alginate-catechol with the $NaIO_4$ gelation solution. This volume of material was more than 100 times larger than the volume injected into the carotid arteries using a catheter. One group of mice was 6 wk old when injected, and a separate group of mice was 14 wk old when treated. For mice injected with saline or alginate-catechol, the body mass increased equally as they grew, suggesting that the material does not elicit large-scale chronic toxicity. Further toxicity studies, including multiple dosing, will be needed to give a better estimate of acute toxicity to specific organs (1).

Subcutaneous Injection of Polymers and Noninvasive Imaging of Inflammation. To further quantify the level of local inflammation that the gel induces over time, particularly at earlier time points, the alginate-catechol gel was injected into the s.c. region of eight hairless immuno-competent SKH-1E mice, and early inflammation markers of host response to biomaterials were monitored over time using noninvasive in vivo imaging. Two materials, polycaprolactone (PCL; a positive control for inflammation) and unmodified alginate (a biocompatible material and negative control for severe inflammation), were also injected. Multiple injections (n = 10–12 replicates) of each polymer were performed on the back of the hairless mice. Two molecular probes were used to follow inflammation: (*i*) luminol, a probe that oxidizes and exhibit luminescence in the presence of reactive oxygen species during inflammation; and (*ii*) Prosense-680, an activatable probe that exhibits near-infrared fluorescence in the presence of cathepsins, a class of inflammatory proteases. The bioluminescence and fluorescence of these probes in the tissue around the injected materials were monitored for 14 d using noninvasive in vivo imaging with an IVIS-Spectrum measurement system (Xenogen). The oxidized alginate-catechol showed the same low level of inflammation as unmodified alginate, whereas polycaprolactone, a material known to elicit moderate amounts of inflammation, induced significantly higher activities of reactive oxygen species and inflammatory proteases (Fig. S1 *E–I*). After 14 d, histological sections of these tissues and polymer were collected. Representative H&E histology sections (Fig. S1 *J–L*) of the retrieved polymer show extensive cellular infiltration and collagen deposition between polycaprolactone particles, whereas the alginate-catechol induced minimal host response, comparable to that of unmodified alginate.

The procedures used for testing the inflammatory response of alginate-catechol s.c. using noninvasive imaging were based on the procedures we previously reported (2–4). The following is a summarized version of that procedure with slight modifications. To inject the solid alginate and alginate-catechol s.c., the alginates were formulated into spherical microcapsules using a microdroplet generator. Before droplet formation, alginate-catechol (without steroid and fluorescent particles) was mixed with the solution containing $NaIO_4$ (described above) to oxidize the catechol moieties and initiate cross-linking. This solution turned dark orange, indicating that oxidation had occurred. The solution was injected through the droplet generator shortly before cross-linking was complete and while it was still a liquid. After the alginate solutions were formed into droplets, they were collected in a solution of 100 mM $CaCl_2$ and incubated for 10 min to allow cross-linking to complete. They were then washed three times with a sterile 0.9% sodium chloride solution. Before s.c. injection of the polymers, mice were kept under inhaled anesthesia using 1–4% isoflurane in oxygen at a flow rate of 2.5 L/min. Lyophilized PCL microparticles were suspended in sterile 0.9% (wt/vol) sodium chloride at a concentration of 67 mg/mL. Hydrogel capsules of alginate or alginate-catechol were also suspended in sterile 0.9% (wt/vol) sodium chloride at an approximate volume percentage of 75%. A volume of 150 μL of PCL particles suspension or hydrogel capsules was injected s.c. via a 23-gauge needle on the back of hairless immunocompetent SKH-1E mice. Hairless mice were used to reduce autofluorescence and absorbance that is caused by hair and interferes with imaging. Mice were started on a nonfluorescent alfalfa-free diet (Harlan Teklad) 3 d before s.c. injections of polymer and maintained on this diet until the desired time point for tissue harvesting. To monitor cathepsin activity, the imaging probe ProSense-680 (PerkinElmer), at a concentration of 2 nmol in 150 μL of sterile PBS, was injected into the mouse tail vein. After 24 h, in vivo fluorescence imaging was performed with an IVIS-Spectrum measurement system (Xenogen). The animals were maintained under inhaled anesthesia using 1–4% isoflurane in oxygen at a flow rate of 2.5 L/min. Whole-animal near-infrared fluorescent images were captured at an excitation of 605 nm and emission of 720 nm. To monitor the concentration of reactive oxygen species,

a volume of 200 μL of sodium luminol (Sigma Aldrich) dissolved in PBS buffer at a concentration of 50 mg/mL was injected i.p. to each mouse before imaging (dose of 500 mg/kg). Ten minutes after this injection, the luminescence from the mouse was imaged using the IVIS system. Data were analyzed using the manufacturer's Living Image 3.1 software. Fluorescent images are presented in fluorescence efficiency, which is defined as the ratio of the collected fluorescent intensity normalized against an internal reference to account for the variations in the distribution of incident light intensity. Regions of interest (ROIs) were selected that included the entire site of injection. ROI signal intensities were calculated in total fluorescent efficiency for fluorescence images and in photons per second for bioluminescent images. After 14 d, mice were killed via CO_2 asphyxiation. The injected polymer and 1-cm^2 full-thickness dermal tissue surrounding the implant were excised, placed in histology cassettes, and fixed in 10% formalin overnight. Following fixation, the tissues were dehydrated by transferring the cassettes to 70% ethanol solutions. The polymer particles with surrounding fixed tissues were embedded in paraffin and sectioned into samples of 5 mm thickness. These samples were stained with H&E for histological analysis.

Assessing Toxicity After Carotid Arteries Were Coated by Measuring Serum Concentrations of Cytokines and Liver Enzymes and Analyzing Histology of Organs. To test whether the treatments induced systemic toxicity or local toxicity in organs, the arteries of mice were coated with the hydrogels, and several measurements for toxicity were determined, including measurements for liver toxicity, cytokine release, and histology of key organs. Four conditions were compared in WT (C57BL/6J) mice:

i) alginate-catechol (nondegradable) coated on the common carotid artery via catheter ($n = 3$),
ii) a negative control with surgery, using the same catheter-based procedure without alginate-catechol (an equivalent volume of PBS was injected through the catheter) ($n = 3$),
iii) a positive control for brain embolisms, inflammation, and toxicity consisting of large fluorescent microbeads (45-μm-diameter latex beads) injected into the carotid via catheter without adhesive hydrogel ($n = 3$), and
iv) a negative control with untreated mice that did not undergo surgery ($n = 4$).

Serum was analyzed at 1 and 7 d after surgery. Serum samples collected 1 d after the experiment were pooled together to obtain a volume sufficient for testing. After 7 d, the mice were killed. At this time point, the serum was collected immediately before killing each mouse and was not pooled. Cytokine concentrations in the serum were determined using multianalyte profiling with immunoassays (Fig. S2 *A*–*C*). Serum was analyzed by Myriad RBMfor cytokine concentrations. Liver toxicity was determined by measuring concentrations of aspartate aminotransferase (AST) and alanine aminotransferase (ALT) in the serum (Fig. S2*D*). Serum was analyzed by Charles River Laboratories for AST and ALT. Histological sections of the brain, kidney, lungs, and liver were prepared as described below (Fig. S3).

We did not find evidence of toxicity in mice treated with alginate-catechol. There were no significant differences in the level of toxicity markers between mice treated with alginate-catechol and mice treated with saline alone, analyzed by ALT and AST levels, cytokine production, and organ histology. Cytokine levels were elevated in all treatment and control groups the day following surgery, as expected after a surgical procedure, and there were no significant differences between the groups at that time. One week after treatment, the cytokine levels from the group treated with large microbeads (i.e., the positive control group) were significantly higher than the other groups. In contrast, there were no significant differences in cytokine levels between mice treated with alginate-catechol and mice treated with saline, supporting the notion that alginate-catechol does not elicit a strong inflammatory or immune response. The AST and ALT values were similar and not significantly different in mice treated with alginate-catechol compared with mice treated with saline, although the values were highly variable. The high variability was likely associated with the response to surgery. Additional data were obtained from apoE$^{-/-}$ mice that had been treated with alginate-catechol or saline in their carotid arteries, and the AST and ALT values were similar and not significantly different. The histological sections of the livers, lungs, kidneys, and brains were morphologically similar between C57BL/6 mice treated with alginate-catechol or saline, and we did not find evidence of toxicity (Fig. S3). Histological sections of the brain did not show evidence of stroke. Supporting these data, none of the treated mice displayed neurological deficits measured using the Bederson scale (5).

Mice treated with hyaluronan-catechol (coated on the common carotid artery and containing 100-nm fluorescent nanoparticles) did not show evidence of stroke, analyzed by histology and the Bederson scale (Fig. S3*B*) (5). Hyaluronan-catechol degrades in the vasculature on the time scale of days (Fig. S8). The cytokine profile of mice treated with hyaluronan-catechol was similar to mice treated with saline or alginate-catechol and did not resemble the cytokine profile of mice treated with large, embolizing microbeads (Fig. S2 *A* and *B*), further supporting the notion that hyaluronan-catechol did not induce stroke. Although we did not find evidence of stroke, we envision that strategies could be used to further ensure that degradable hydrogels do not detach in future applications of this technology. One approach would be to use hydrogels that degrade more slowly than the time required for the hydrogel to become encapsulated by endothelial cells (time scale of weeks). In this way, pieces of degraded materials would be shielded from entering the blood stream by the endothelium and the fibrous cap. Controlling the mechanism of degradation by favoring materials that degrade by surface erosion rather than bulk degradation will also help prevent detachment of material. It is important to note that alginate-catechol is biostable and degrades on the time scale of months to years, at which time it is encapsulated by cells and would not detach.

Testing the Potential of Alginate-Catechol to Clot Blood. In all mice tested, occlusion of blood flow was never observed in the treated vessels, including mice treated for less than 1 wk, 1 mo, or 4 mo. We closely observed mice, and no stroke symptoms were detected. Additionally, intravascular coagulation was never seen in the treated area. The potential of the hydrogel to initiate blood coagulation was further analyzed in two separate ways: (*i*) histological sections were stained for activated platelets (antigen CD41) and (*ii*) the clotting time of plasma exposed to the hydrogel was determined (Fig. S6). As a positive control for coagulation, the carotid artery of a mouse was ligated overnight, which led to the formation of a clot. In this positive control, histological analysis showed a high density of platelets on the vessel wall and platelets spread throughout the clot (Fig. S6*B*). In contrast, a vessel that was coated with the hydrogel for 30 d showed no platelet deposition or thrombus when stained for CD41 (Fig. S6*A*).

To test whether alginate-catechol is an initiator of blood coagulation, either as a cross-linked hydrogel or when dissolved (not cross-linked), the clotting time of plasma exposed to the hydrogel and non–cross-linked alginate-catechol was determined (Fig. S6*C*), using previously described procedures (6, 7). As a positive control for coagulation, samples of plasma were exposed to single piece of glass (20 mg of a glass coverslip; Fisher Scientific). Glass is an initiator of coagulation via the factor XII pathway of coagulation (8). Pooled normal plasma (citrated) was obtained from Affinity Biologicals. This plasma contained platelets, but lower concentrations than whole blood—it is considered platelet poor

but not platelet free. This citrated plasma was recalcified by adding a solution containing 40 mM $CaCl_2$ and 90 mM NaCl. The plasma and the solution containing $CaCl_2$ and NaCl were gently mixed 3:1 by volume. To test the clotting time of plasma on various substrates, recalcified plasma (266 μL) was added to 1.5-mL plastic tubes containing either a piece of glass, alginate-catechol hydrogel, dissolved alginate-catechol (not cross-linked), or no substrate. Each tube contained 20 mg of either glass or hydrogel (hydrated, 3.75% solids). The glass was oxidized by treating both sides of a coverslip for 30 min with deep UV light, using a UV cross-linker apparatus (Spectrolinker; Spectronics Corporation). The oxidized glass was broken with forceps, and a single 20-mg glass piece was placed in each tube. To determine clotting times, the tubes of plasma were continuously inverted slowly using a rotating apparatus (Labquake shaker; Labindustries). In the positive control samples, plasma exposed to glass clotted in 13 ± 0.5 min, whereas plasma alone, alginate-catechol hydrogel, and non–cross-linked alginate-catechol did not clot in the observed period (35 min). This long clot time indicates that the material is not a direct initiator of coagulation (7).

SI Materials and Methods

Synthesizing Alginate-Catechol. Alginate (Protantol LF 10/60; FMC Biopolymer) was purified by dialyzing it against water using membrane tubing (molecular weight cut-off of 6–8 k; Spectrum Laboratories) overnight. Purified alginate was recovered by freeze-drying the solution. Alginate-catechol was synthesized by activating the carboxy groups of alginate and reacting them with the amino groups on dopamine, a catechol-containing molecule. Purified alginate (400 mg) was dissolved in 80 mL of a buffer consisting of 0.1 M 2-(*N*-morpholino)ethanesulfonic acid (Mes) at pH 5.9. Nitrogen gas was bubbled through the solution during dissolution to remove oxygen gas. After the alginate dissolved, *N*-(3-dimethylaminopropyl)-*N*′-ethylcarbodiimide hydrochloride (EDC) (437.1 mg; Sigma-Aldrich) and *N*-hydroxysulfosuccinimide sodium salt (sulfo-NHS) (495.1 mg; Sigma-Aldrich) were each dissolved in 2 mL of Mes buffer and added to the alginate solution. The solution was stirred for 30 min, and then 3-hydroxytyramine hydrochloride (dopamine) (432.4 mg; Sigma-Aldrich) was dissolved in 2 mL of Mes buffer and added to the alginate reaction mixture. The reaction mixture was stirred for 1 h to produce alginate-catechol. Purification of alginate-catechol was accomplished by dialyzing the reaction mixture against water (spectra/por membrane tubing; MWCO 6–8 k) three times for a total of 24 h of dialysis. The solution was then concentrated using centrifugal filters (CentriPrep, MWCO 10,000 kDa; Millipore) by centrifuging at 800 × *g* until the volume was reduced to 25 mL. Alginate-catechol was further purified using centrifugal desalting columns (PD-10; GE Healthcare) using the vendor's procedure. Water was removed from the sample by freeze-drying. The yield was 189 mg of a white fluffy solid. Incorporation of dopamine into alginate was confirmed by the appearance of amide bonds in FTIR spectroscopy measurements (absorbance at 1,730 cm^{-1}, Alpha-T FTIR; Bruker). Measuring the absorbance at 280 nm by ultraviolet-visible spectroscopy (Cary 50 Bio UV-Visible Spetrometer; Varian) indicated that ∼1–2% of the saccharide units were modified with catechol. Synthesis of the desired product was further confirmed by H^1 NMR (Fig. S1*A*). To prepare hyaluronan-catechol, the above procedure was used, replacing alginate with hyaluronic acid (HA) (molecular weight, 450 kDa; Genzyme). Hyaluronan-catechol has been prepared previously (9). The following quantities were used: 400 mg HA, 437 mg EDC, 495 mg sulfo-NHS, and 432 mg dopamine.

Gelation of Adhesive Hydrogels. Alginate-catechol or hyaluronan-catechol was dissolved in PBS (pH 7.4) (5% wt/vol for alginate-catechol or 2.5% for hyaluronan-catechol). A gelation solution was prepared to induce cross-linking of the alginate-catechol or hyaluronan-catechol macromers. The gelation solution was prepared by combining 100 μL of a solution of sodium periodate ($NaIO_4$, 10 mg/mL in PBS; Sigma-Aldrich), 20 μL of a solution of suspended fluorescent nanoparticles to visualize the gel using fluorescence imaging (100 nm diameter, emission at 750 or 200 nm diameter, emission at 680 nm in a solution of 2% solids; Invitrogen), and a solution of NaOH (0.4 M, 12 μL added to the alginate-catechol gelation solution or 1 μL added to the hyaluronan-catechol gelation solution). The alginate-catechol or hyaluronan-catechol solution and gelation solution were mixed in a ratio of 3:1. Immediately after the solutions were mixed, the solution turned brown, indicating that the catechol moieties were oxidized. The solution gelled in 10–20 min. Using pH paper, the pH of the alginate-catechol mixture during gelation was ∼8.5. The gelation time could be varied by adjusting the amount of NaOH that was added and could be decreased to <20 s for hyaluronan-catechol.

A solution of 5% unmodified alginate (no catechol) in PBS did not gel when this $NaIO_4$ solution was added to it. Solutions of unmodified alginate were gelled by adding a solution of $CaCl_2$ (200 mM in H_2O) to it in a ratio of 3:1 alginate:$CaCl_2$ solution.

In experiments where other agents were incorporated into the gel, these agents were added 1 min after the alginate-catechol solution and $NaIO_4$ gelation solution were mixed. In experiments where degradable poly(lactic-coglycolic acid) (PLGA) particles were incorporated into the hydrogel (data in Fig. 3), 10 mg of solid particles was suspended in 100 μL PBS, and then this solution was added to the alginate-catechol solution in a 1:10 ratio. In experiments treating atherosclerotic plaques (data in Fig. 5 *A*–*K*), fluorescent microparticles were not included in the hydrogel, but a soluble fluorescent dye, Prosense 680 Control (8 μM in the hydrogel; Visen), was added to image deposition of the hydrogel in the artery. In experiments treating atherosclerotic plaques, a steroid, dexamethasone 21-phosphate disodium salt (5 μg/μL in the hydrogel; Sigma-Aldrich), was incorporated into the hydrogel.

The hyaluronan-catechol hydrogel was degraded when a solution of hyaluronidase was added to it. The hydrogel (50 μL) was formed in a 1.5-mL tube and then submerged in a solution of hyaluronidase (1 mL, 10,000 U/mL in PBS, from bovine testes; Sigma-Aldrich). The hydrogel degraded within 24 h. The hydrogel did not degrade when submerged in PBS alone. The alginate-catechol solution did not degrade in this solution of hyaluronidase.

Culturing HUVECs. HUVECs (Lonza) were cultured in Endothelial Cell Growth Medium-2 (Lonza), adhered in cell culture–treated flasks (BD Falcon). Cells were passaged by rinsing with PBS, incubating with Trypsin-EDTA (0.05%) for 5 min, suspending them in growth medium to neutralize trypsin, and then pelletting by centrifugation. The pellet of cells was then resuspended in media, counted with trypan blue, and seeded on a new cell culture–treated flasks.

Measuring the Adhesive Strength of Alginate-Catechol In Vitro. The adhesive ability of alginate-catechol was first characterized by coating the hydrogel on endothelial cell–lined microfluidic channels and determining the shear rate at which the hydrogel detached from the cells. Microfluidic devices were fabricated by rapid prototyping in polydimethylsiloxane (PDMS, Sylgard 184 Silicone Elastomer Kit; Dupont) using SU-8 photoresist masters (10). The square-shaped channels of the device had heights of 700 μm. To prepare the devices to support cell growth, the fabricated devices were soaked overnight in PBS under vacuum, autoclaved, and then filled with 100 μL of a solution of fibronectin (100 μg/mL in PBS; Sigma-Aldrich) and incubated for 4 h at 37 °C, 5% CO_2. After the channels were coated with fibronectin, the device was rinsed with PBS and filled with 100 μL of HUVECs at a concentration of 500,000 cells/mL in growth media. The device was incubated for 3 h to allow the cells to attach to the channel walls. The device was then connected to a syringe pump (Harvard Apparatus PHD 2000), and

growth medium was flowed through the device overnight at 0.5 μL/min, allowing the cells to grow and spread under flow. The device and cells were kept at 37 °C with 5% CO_2 during these incubation steps. Just before the adhesion experiment, the cells were stained blue with Hoechst nucleus stain dye to allow visualization with fluorescent imaging. To coat the walls of the device with hydrogel, one end the device was cut off to allow a catheter to be inserted into it. The catheter was composed of modified polytetrafluoroethylene (PTFE) tubing (inner diameter, 150 μm; outer diameter, 310 μm; Zeus) that was sealed at the end and had small (~5 μm) holes punched into its side. The holes spanned a length of ~250 μm and began ~250 μm from the tip. This tubing was connected to larger-diameter tubing (inner diameter, 4 mm; outer diameter, 5.5 mm; Zeus) that was connected to a 10-μL glass syringe (Hamilton Company). After the catheter was inserted into the device, 0.8–1 μL of either alginate-catechol with the $NaIO_4$ gelation solution or unmodified alginate was mixed with fluorescent particles and injected into the channel via the catheter. When unmodified alginate was injected, 1 μL of alginate with fluorescent particles was injected and then ~50 μL of a $CaCl_2$ solution (200 mM) in water was injected onto the alginate via the catheter to gel the alginate in place. Immediately after the hydrogels were coated on the walls of the device, the device was connected to the syringe pump again, and growth medium was flowed through the device at flow rates between 0 and 50,000 μL/min. The amount of coverage of the hydrogels on the channels was measured by quantifying the fluorescence intensity from images of the hydrogel in the channels, which were taken using a fluorescent microscope (Axiovert 200M; Zeiss).

The adhesive strength of the alginate-catechol hydrogel was also tested in a lap-shear tensile strain test using an Instron 5542 single column testing system (11). The hydrogel solutions were injected between a titanium plate and the endothelium of a section of a bovine carotid artery. The bovine artery had been excised for 3 d and was rigorously washed, which likely denuded the endothelium. Titanium was used because catechol adhesives are known to bind strongly to titanium (12). The carotid artery was glued to a glass plate with super glue (Permatex). The two plates were inserted into clamps on the Instron system such that the plates were parallel, and the surface overlap between the titanium and carotid artery covered by the hydrogel was 13 × 18 mm. A 100-μL solution of unmodified alginate or alginate-catechol was injected between the two plates. The hydrogel solutions were gelled following addition of the gelation solutions, and then the plates were pulled away from each other, remaining parallel to each other and maintaining their separation distance, at an extension rate of 3.3 μm/s. Failure of the hydrogel resulted in the hydrogel being detached from the artery while remaining attached to the titanium plate, indicating that adhesive failure occurred rather than cohesive failure or substrate failure.

Gelation In Situ in the Arteries of Living Mice. Experimental protocols were in accordance with National Institutes of Health guidelines for the humane care and use of laboratory animals, the Massachusetts Institute of Technology Committee on Animal Care, and the Massachusetts General Hospital Subcommittee on Research Animal Care and the Institutional Animal Care and Use Committee. Female apoE$^{-/-}$ mice and C57BL/6J mice were purchased from the Jackson Laboratory at 8–10 wk of age. In experiments using apoE$^{-/-}$ mice (data in Figs. 4 and 5), the mice were 21–24 wk old at the time of surgery and had been kept on a high-cholesterol diet (Harlan Laboratories) since they were 8–10 wk of age. The mice had substantial plaque growth at the time they were initially treated. In apoE$^{-/-}$ mice, a fluorescent substrate for proteases in atherosclerotic plaques, Prosense 680 or Prosense 750 (2 nmol; Visen), was added 18–24 h before surgery to visualize the plaque during hydrogel deposition (Fig. 4 *A*–*N* but not Fig. 5 *L* and *M*).

The neck of anesthetized mice (2% isofluorane in 2 L/min oxygen) was shaved, and a hair-degrading agent (Nair) was applied for complete hair removal. The surgical field was then swabbed with isopropyl alcohol and betadine. Under a dissecting microscope, a vertical (10 mm) incision was made on the right neck, and the common carotid artery (CCA), internal carotid artery (ICA), and external carotid artery (ECA) were identified and isolated. Two sutures of 8-0 mononylon (Ethicon; Johnson & Johnson) were placed around the ECA, one around the ICA, and one around the CCA. At this time, the alginate-catechol and gelation solutions (including fluorescent particles, degradable microspheres, and/or dexamethasone) were mixed and filled into a catheter. The catheter was composed of modified PTFE tubing (inner diameter, 150 μm; outer diameter, 310 μm; Zeus) that was sealed at the end and had small (1–30 μm) holes punched along its side 0.1–1 mm from the tip. This tubing was connected to larger-diameter tubing (inner diameter, 4 mm; outer diameter, 5.5 mm; Zeus) that was connected to a 10-μL glass syringe (Hamilton Company). A glass microsyringe with a reinforced metal plunger and a maximum volume of only 10 μL was used to control the amount of solution injected (0.3–0.6 μL) on a microliter scale.

For deposition of the gel in the CCA (data in Fig. 2 and Figs. S2–S6 and S8), a temporary ligation was made on the proximal portion of the CCA and at the distal portion of ICA to stop the blood flow. The distal suture around the ECA was permanently tied off, and the second suture was kept loose to secure the catheter. The ECA was opened using delicate scissors. A catheter filled with PBS was inserted into the ECA and moved into the CCA, and 5–10 μL of saline was injected to flush blood from the region. The catheter containing saline was removed, and a second catheter containing the pregel solution was inserted to the desired location in the CCA and secured. The pregel (0.3–0.6 μL) was injected from the catheter. The pregel accumulated in the annular region between the catheter and the vessel wall (Fig. S4*A*) To estimate when the pregel would fully cross-link in vivo, a small sample of the pregel was put aside before injection and monitored for gelation. This sample was allowed to fully cross-link and adhere for 30 min, and then the catheter was removed, leaving a film of hydrogel 10–100 μm thick adhered to the vessel wall. After the catheter was removed, the ECA was tied off, and blood flow was restored after releasing the sutures of the ICA and CCA. In experiments where microbeads were injected as a positive control for inflammation and toxicity (data in Fig. S2), 100 beads were injected in 0.3–0.6 μL of PBS. The beads had an average diameter of 45 μm and fluorescent emission at 486 nm (Polysciences).

When determining the optimum injection volume, we estimated that 0.3 μL (equal to 0.3 mm^3) would be needed to coat a 100-μm-thick layer of gel on a 1-mm-long section of vessel with an inner circumference of 3 mm.

For deposition of the gel in the ECA and the bifurcation of the ICA and ECA (data in Figs. 3–5 and Figs. S7 and S9), the proximal portion of the CCA and the distal portion of the ICA and ECA were temporary ligated to stop the blood flow. A small hole was made at the anterior wall of the CCA (using a 31-gauge needle), allowing the catheter to be inserted into the CCA and moved to the ECA or ICA/ECA bifurcation at the site of the plaque and secured. The same catheter and procedure described above was used in apoE$^{-/-}$ mice to deposit (0.3–0.6 μL) of the pregel. The pregel solution was injected and allowed to gel. The hole at the CCA anterior wall was closed using two to three sutures of mononylon 10-0. The blood flow was restored after the sutures were released at the ECA, ICA, and CCA.

The presence of the gel in vivo was confirmed using an Olympus OV110 Small Animal Imaging System. Images were taken using separate filters that allowed detection of emitted light at 500, 680, and 750 nm to detect the Prosense substrate, submicron particles in the hydrogel, and BODIPY when incorporated into the hydrogel. Images were false-colored: light in the near-infrared wavelengths were false-colored as green, yellow, or pink, as indicated in the

figure legends. After imaging, the surgical wound was closed using 7-0 mononylon sutures. At different time points (between 3 d and 4 mo after imaging), the carotid arteries were surgically reexposed, and the gel was reimaged. At this time, mice were killed, and carotid arteries were excised for histological analysis. Imaging inflammation with the cathepsin substrate was used to locate the plaque, but this imaging method could not be used to quantify the extent of inflammation over time because of the surgical procedure required in these experiments. There was variable and high background signal from the fluorescent agent in tissue adjacent to the vessel. This signal was due to inflammation in the healing response following the surgical procedure, which exposed tissue surrounding the vessel both in mice treated with the gel and control mice that underwent surgery without gel. For these reasons, we relied on histological analysis and qPCR to assess inflammation.

In experiments comparing histology from treated and untreated apoE$^{-/-}$ carotid arteries (data in Fig. 5 *A–K*), mice were treated in the carotid artery on one side of the mouse, whereas the other carotid artery was not treated. Ten apoE$^{-/-}$ mice were treated with alginate-catechol containing steroids, and three were treated with the same catheter-based procedure without alginate-catechol (an equivalent volume of PBS containing an equivalent concentration of dexamethasone was injected through the catheter). In each mouse, the treated and the untreated carotid arteries were collected and analyzed in a blinded fashion.

In experiments comparing the concentration of cytokines and inflammatory markers in apoE$^{-/-}$ mice (data in Fig. 5 *L* and *M* and Fig. S2), five apoE$^{-/-}$ mice were treated with alginate-catechol containing steroids, and five other mice were treated with the same catheter-based procedure without alginate-catechol (an equivalent volume of PBS but no steroid was injected through the catheter). Serum and carotid arteries were collected after 1 wk. The concentrations of NF-κB (NCBI Gene ID: 18033) and matrix metallopeptidase-9 (MMP-9) (NCBI Gene ID: 17395) in the arteries were measured using quantitative real-time PCR. The tissues were excised and stabilized using RNA-stabilizing solution (RNAlater; Ambion) and then stored at 4 °C until use. mRNA was extracted from the tissues using a RNA extraction kit (RNeasy Micro; Qiagen) using the manufacturer's instructions and then converted to cDNA (high capacity RNA-to-cDNA kit; Applied Biosystems). qPCR was conducted using a Taqman assay (Applied Biosystems) and a real-time PCR machine (AB 7300; Applied Biosystems). GAPDH served as loading control. The concentrations of cytokines in the serum were determined by outsourcing to Myriad RBM, where the concentrations were measured using a protocol for multianalyte profiling approved by the Clinical Laboratory Improvement Amendments (CLIA; federal regulatory standards that apply to all clinical laboratory testing).

Histology of the Excised Vessels. Excised carotid arteries were embedded in optimal cutting temperature (OCT) compound (Sakura Finetek). Fresh-frozen 5-μm-thick serial tissue sections were cut at the bifurcation of the ICAs and ECAs to ∼1 mm downstream in the ECA. The sections were stained with H&E to assess overall morphology. The adjacent sections were stained for endothelial cells, smooth muscle cells, macrophages, or vascular adhesion molecule 1 (VCAM-1). Immunofluorescence staining was carried out using CD31 (platelet endothelial cell adhesion molecule-1): clone MEC13.3 (BD Biosciences), smooth muscle actin (SMA) (NeoMarkers), and CD107b (MAC-3): clone M3/84 (BD Biosciences), followed by the appropriate biotinylated secondary antibodies (Vector Laboratories) and streptavidin-Texas red (GE Healthcare). The slides were coverslipped using a mounting medium with DAPI (Vector Laboratories) to identify the nuclei. Images were captured and processed using a fluorescent microscope (Axiovert 200M; Zeiss). For immunohistochemistry, the tissue sections were stained for SMA (NeoMarkers), VCAM-1: clone: 429 (MVCAM.A, from purified rat anti-mouse CD106/VCAM-1; BD Biosciences), CD11b: clone M1/70 (BD Biosciences), and CD41: clone MWReg30 (BD Biosciences). The reaction was visualized using biotinylated secondary antibodies (Vector Laboratories), a Vectastatin ABC kit (Vector Laboratories), and AEC substrate (Dako). All sections were counterstained with Harris hematoxylin, and images were digitized automatically using a NanoZoomer 2.0RS microscope (Hamamatsu).

Statistical Analysis. The *P* values reported in Figs. 2*D* and 5 *B, C, L,* and *M* were calculated using the Student *t* test (two-tailed test for two samples with unequal variance). The *P* value reported in Fig. 5*A* was calculated using the Wilcoxon signed-rank test (two-tailed). Because of the nonnormal distribution of the sample set in Fig. 5*A*, the Wilcox signed-rank test was used to determine the statistical significance of the alginate-catechol treatment on smooth muscle thickness in the plaques. The *P* value using the Wilcoxon test was 0.0001, whereas the *P* value calculated using the Student *t* test (two-tailed test for two samples with unequal variance), which is appropriate only for data that have a normal distribution, was 0.0015.

Releasing Small Molecules from Alginate-Catechol. To test whether small molecules could be directly released from alginate-catechol in vitro, dexamethasone 21-phosphate disodium salt (dexamethasone) was added to the hydrogel (as described above), and the amount of dexamethasone released at various times was measured. In four 15-mL tubes, 50 μL of the alginate-catechol hydrogel containing 0.5 mg of dexamethasone was cross-linked and submerged under 5 mL PBS. Solutions with known concentrations of dexamethasone were also prepared. At various time points, 200-μL aliquots were taken from the supernatant and frozen at −20 °C. The concentration of dexamethasone in the samples was measured using two different methods. The concentration was measured using HPLC, by comparing the absorbance at a specific retention time to stock solutions of dexamethasone (data in Fig. 3). To validate this result, the concentration of dexamethasone over time was determined using an ELISA for dexamethasone (Fig. S9*C*), following the protocol given by manufacturer of the ELISA kit (Neogen). The rate of release of dexamethasone from the hydrogel, determined using the ELISA kit, was similar to the rate of release determined using HPLC.

To test whether small molecules could be released from degradable particles blended into the hydrogel, a fluorescent dye, 4,4-Difluoro-1,3,5,7,8-Pentamethyl-4-Bora-3a,4a-Diaza-s-Indacene (BODIPY), was incorporated into PLGA particles and blended with alginate-catechol before gelation. Procedures for preparing PLGA particles containing small molecules have been previously described (13, 14). A solution was prepared containing BODIPY (1 mg; Invitrogen), and PLGA (300 mg, lactide/glycolide ratio of 50:50; Lactel/Durect) in 7.5 mL dichloromethane (DCM; Sigma-Aldrich). A solution of 1% polyvinyl alcohol (Polysciences) in H_2O was prepared by dissolving the polyvinyl alcohol (PVA) overnight at 100 °C. To form microdroplets, the PLGA/BODIPY/DCM solution was added rapidly to 50 mL of the PVA solution via a syringe and needle while the solutions were subjected to homogenization (model L4RT-A; Silverson) for 1 min at 6,000 rpm. The resulting mixture was added to 100 mL deionized water and stirred for 15 min on a stir plate. The DCM was then removed from the mixture by rotary evaporation (R-200; Buschi), resulting in the formation of solid particles of PLGA/BODIPY suspended in the aqueous PVA solution. The particles were washed three times in H_2O by centrifuging the mixture at 1,800 × *g* for 2 min, removing the aqueous supernatant from the pellet of particles, and resuspending the particles in 5 mL H_2O. The bright green particles were isolated from clear H_2O by freeze-drying the mixture. The diameter of the particles were 2–25 μm, which was measured by suspending the particles in PBS, imaging the particles using a microscope

(Axiovert 200M; Zeiss), and quantitatively comparing their size to images of a microruler (Ted Pella).

To measure the rate of release of BODIPY from alginate-catechol in vitro, three hydrogel samples (35 μL) containing 1% BODIPY/PLGA particles were cross-linked in the bottom of three 15-mL tubes and then submerged under 2.4 mL PBS. Solutions containing the same concentration of BODIPY/PLGA particles in PBS, without the alginate-catechol hydrogel, were also prepared. At various time points, 150-μL aliquots were taken from the supernatant and frozen at −20 °C. The fluorescence intensity of these samples was measured using a fluorescence plate reader (Perkin-Elmer). The release of BODIPY from the alginate-catechol in vivo was detected by analyzing histological sections of vessels coated with the hydrogel. Green fluorescence was detected in the vessel wall near particles in the hydrogel. Green fluorescence was also observed in the same region of the vessel in adjacent sections that did not contain the same particles, indicating that the fluorescence in the vessel did not accumulate after the section was cut (Fig. S9 *A* and *B*).

1. Gad SC (2007) *Animal Models in Toxicology* (CRC Press, Boca Raton, FL), 2nd Ed, p 54.
2. Bratlie KM, et al. (2010) Rapid biocompatibility analysis of materials via in vivo fluorescence imaging of mouse models. *PLoS ONE* 5(4):e10032.
3. Dang TT, et al. (2011) Spatiotemporal effects of a controlled-release anti-inflammatory drug on the cellular dynamics of host response. *Biomaterials* 32(19):4464–4470.
4. Liu WF, et al. (2011) Real-time in vivo detection of biomaterial-induced reactive oxygen species. *Biomaterials* 32(7):1796–1801.
5. Bederson JB, et al. (1986) Rat middle cerebral artery occlusion: Evaluation of the model and development of a neurologic examination. *Stroke* 17(3):472–476.
6. Kastrup CJ, Shen F, Runyon MK, Ismagilov RF (2007) Characterization of the threshold response of initiation of blood clotting to stimulus patch size. *Biophys J* 93(8): 2969–2977.
7. Butenas S, Bouchard BA, Brummel-Ziedins KE, Parhami-Seren B, Mann KG (2005) Tissue factor activity in whole blood. *Blood* 105(7):2764–2770.
8. Kastrup CJ, Runyon MK, Shen F, Ismagilov RF (2006) Modular chemical mechanism predicts spatiotemporal dynamics of initiation in the complex network of hemostasis. *Proc Natl Acad Sci USA* 103(43):15747–15752.
9. Lee H, et al. (2008) Substrate-independent layer-by-layer assembly by using mussel-adhesive-inspired polymers. *Adv Mater (Deerfield Beach Fla)* 20(9):1619–1623.
10. Anderson JR, et al. (2000) Fabrication of topologically complex three-dimensional microfluidic systems in PDMS by rapid prototyping. *Anal Chem* 72(14):3158–3164.
11. ASTM Committee on Material Test Methods (2003) *Standard Test Method for Strength Properties of Tissue Adhesives in Lap-Shear by Tension Loading. Designation F 2255* (ASTM International, West Conshohocken, PA).
12. Lee H, Dellatore SM, Miller WM, Messersmith PB (2007) Mussel-inspired surface chemistry for multifunctional coatings. *Science* 318(5849):426–430.
13. Cohen S, Yoshioka T, Lucarelli M, Hwang LH, Langer R (1991) Controlled delivery systems for proteins based on poly(lactic/glycolic acid) microspheres. *Pharm Res* 8(6): 713–720.
14. Kohane DS, et al. (2006) Biodegradable polymeric microspheres and nanospheres for drug delivery in the peritoneum. *J Biomed Mater Res A* 77(2):351–361.

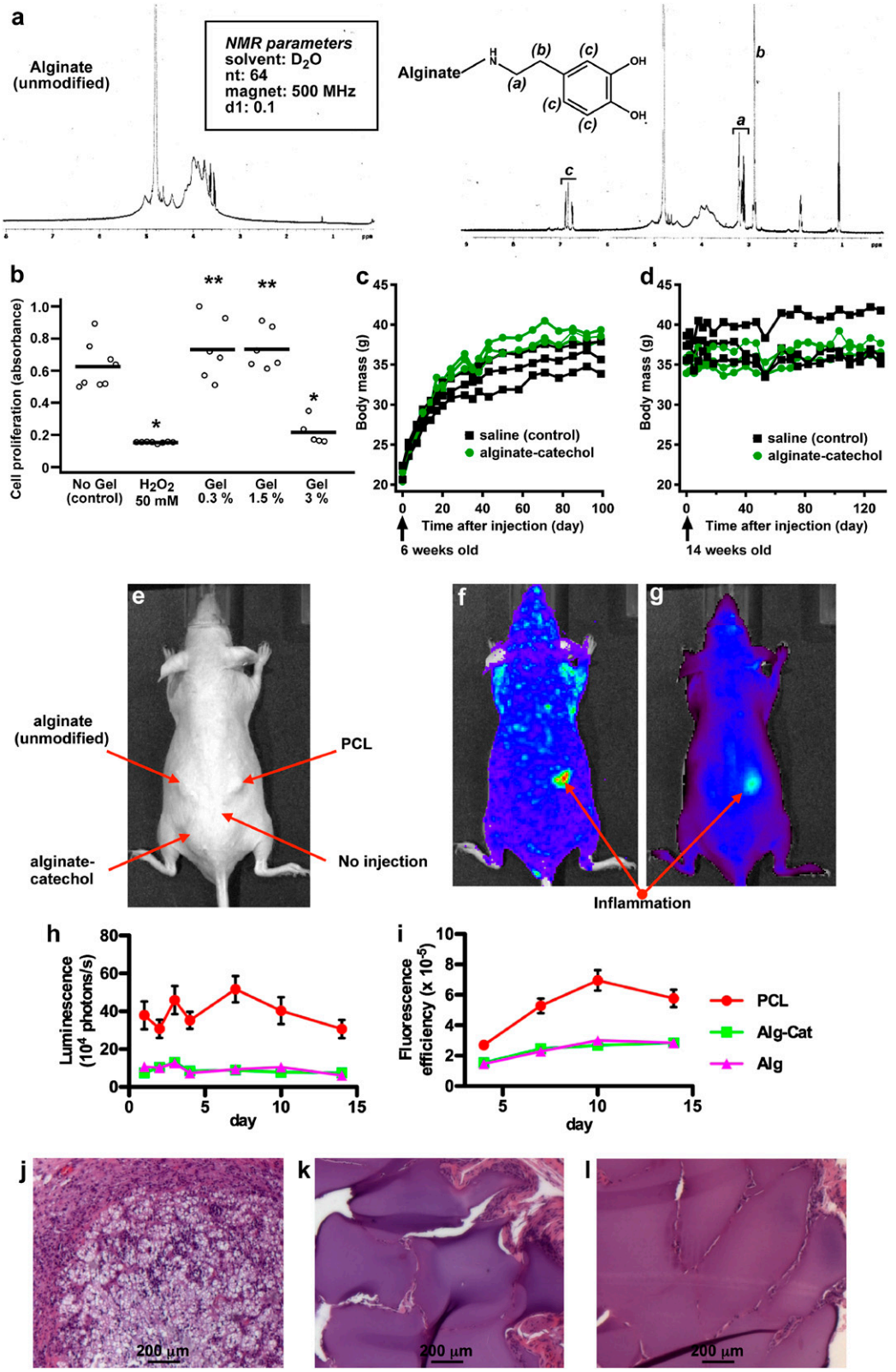

Fig. S1. Measuring in vitro cell proliferation, in vivo body mass change, and inflammation to alginate-catechol injected subcutaneously. (*A*) NMR spectra of unmodified alginate and alginate-catechol. (*B*) In vitro cell proliferation assay comparing HUVECs grown 24 h in solutions containing various amounts of cross-linked alginate-catechol or H_2O_2 (negative control). The hydrogel did not exhibit significant toxicity until the amount of hydrogel was 3% of the total volume (this volume of hydrogel is 20 times greater than the volume injected into the carotid arteries in Figs. 2–5). $*P < 0.05$, $**P > 0.5$ vs. untreated control cells. (*C* and *D*) Comparing the change in body mass of mice following i.p. injections of alginate-catechol hydrogel. Separate groups of mice ($n = 3$) were injected when they were either 6 (*C*) or 14 wk old (d) with 75 μL of either saline (control) or alginate-catechol. (*E*–*L*) s.c. injections of alginate-catechol (Alg-Cat) show a low

Legend continued on following page

inflammatory response, indistinguishable from unmodified alginate (Alg). Polycaprolactone (PCL) served as a positive control for moderate inflammation. (*E*) Injection pattern showing administration sites of different polymers on the back of one representative mouse. (*F*) Luminescence image of luminol oxidized by reactive oxygen species 7 d after administration. (*G*) Fluorescence image of Prosense-680 activated by cathepsin activity in the same mouse on day 7. (*H* and *I*) Time-lapse quantification of the data from *F* and *G* and seven other mice (n = 10–12 injections). (*J–L*) Representative H&E histology sections of polycaprolactone (*J*), alginate-catechol (*K*), and alginate (*L*) retrieved from mice after 14 d.

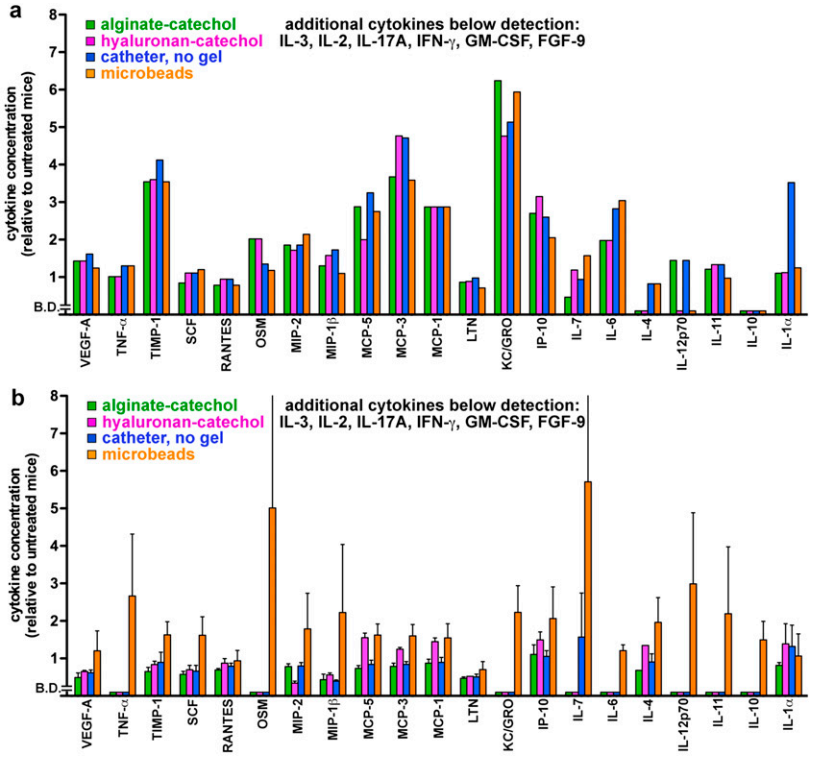

c

Acronym	Biomarker name
VEGF-A	Vascular Endothelial Growth Factor A
TNF-α	Tumor Necrosis Factor alpha
TIMP-1	Tissue Inhibitor of Metalloproteinases 1 Mouse
SCF	Stem Cell Factor
RANTES	T-Cell-Specific Protein RANTES
Oncostatin-M	Oncostatin-M
MIP-2	Macrophage Inflammatory Protein-2
MIP-1 β	Macrophage Inflammatory Protein-1 beta
MCP-5	Monocyte Chemotactic Protein-5
MCP-3	Monocyte Chemotactic Protein 3
MCP-1	Monocyte Chemotactic Protein 1
LTN	Lymphotactin
KC/GRO	Growth-Regulated Alpha Protein
IP-10	Interferon gamma Induced Protein 10
IL-7	Interleukin-7
IL-6	Interleukin-6
IL-4	Interleukin-4
IL-3	Interleukin-3
IL-2	Interleukin-2
IL-17A	Interleukin-17A
IL-12p70	Interleukin-12 Subunit p70
IL-11	Interleukin-11
IL-10	Interleukin-10
IL-1 α	Interleukin-1 alpha
IFN-γ	Interferon gamma
GM-CSF	Granulocyte-Macrophage Colony-Stimulating Factor
FGF-9	Fibroblast Growth Factor 9

d

Carotid surgery	Mouse strain	Treatment	ALT (U/L)	AST (U/L)
No	W.T. (C57BL/6)	No Treatment	28 ± 2	95 ± 13
Yes - 1 week	apoE -/-	Saline	61 ± 9	139 ± 55
Yes - 1 week	apoE -/-	Alginate-catechol	66 ± 80	138 ± 106
Yes - 1 week	W.T. (C57BL/6)	Saline	67 ± 37	130 ± 73
Yes - 1 week	W.T. (C57BL/6)	Alginate-catechol	56 ± 19	74 ± 25
Yes - 1 week	W.T. (C57BL/6)	Microbeads	40 ± 11	186 ± 123
Yes - 24 hr	W.T. (C57BL/6)	Saline	74	248
Yes - 24 hr	W.T. (C57BL/6)	Alginate-catechol	48	164
Yes - 24 hr	W.T. (C57BL/6)	Microeads	106	328

Fig. S2. Quantifying the concentrations of markers of toxicity and inflammation in serum of mice following surgery and carotid treatments (without steroids). (*A* and *B*) Concentrations of cytokines in serum of WT mice 1 d after surgery (*A*) and 1 wk after surgery (*B*). The values were normalized to the average concentration in four untreated mice. Arteries were treated with alginate-catechol (nondegradable hydrogel that adhered to the vessel) ($n = 3$), hyaluronan-catechol (degradable hydrogel that adhered to the vessel) ($n = 2$), saline delivered via the catheter without gel ($n = 3$), and microbeads (45-μm-diameter latex beads delivered without the gel and that did not remain adhered) ($n = 3$). The day after surgery (*A*), the serum from each group of mice was pooled, whereas after 1 wk (*B*), a larger amount of serum was collected from each mouse when it was killed and then measured individually. Data indicate mean ± SEM. (*C*) Acronyms used for biomarkers and cytokines. (*D*) Concentrations of ALT and AST in serum of mice following depositions of alginate-catechol, saline, or microbeads in their carotid arteries. Values indicate mean ± SD in *D*.

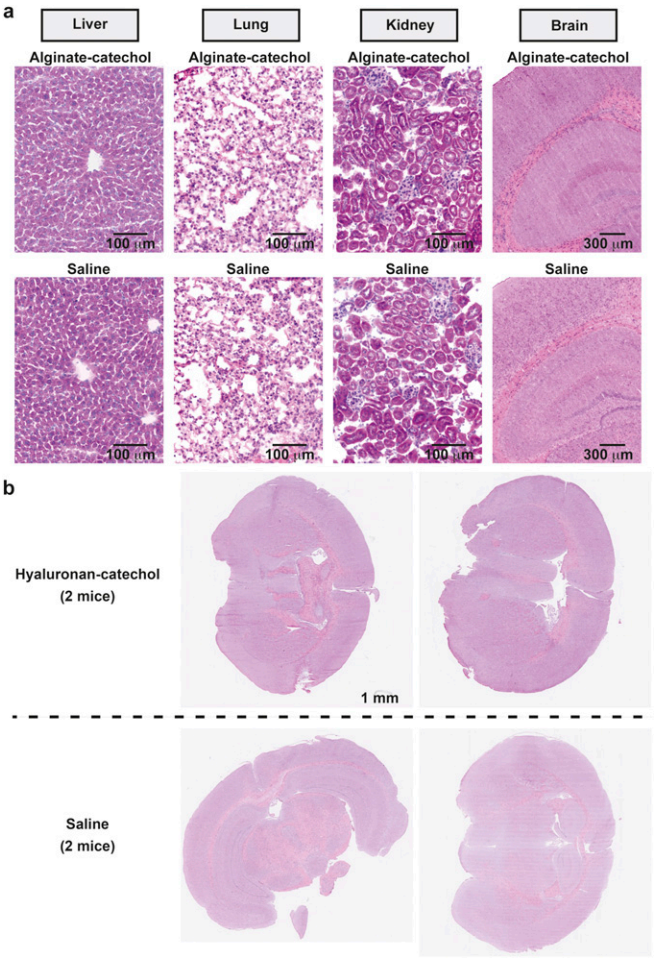

Fig. S3. Histological sections from organs of mice treated with adhesive gels in their carotid arteries. (*A*) Sections from the organs of mice treated with alginate-catechol or saline for 1 wk. (*B*) Brain sections from mice treated with hyaluronan-catechol (degradable gel) or saline for 1 wk show no evidence of stroke.

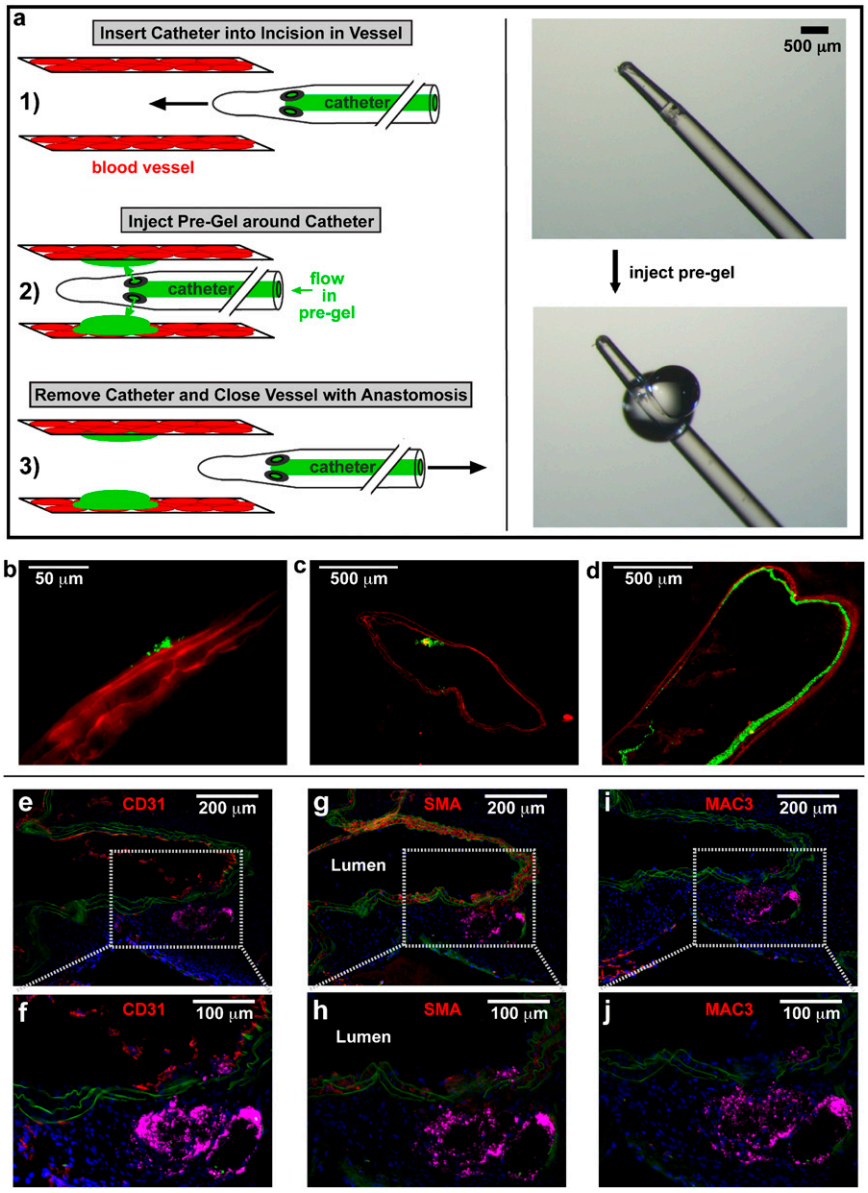

Fig. S4. Deposition and long-term adherence of adhesive gels in the carotid arteries of mice. (*A*) Schematic and micrographs of the catheter-based system used for depositing cross-linkable hydrogels in carotid arteries. (*B–D*) Alginate-catechol can be coated onto blood vessels in various lengths. Overlaid fluorescence images of histological sections of three different carotid arteries (red, autofluorescence) coated with alginate-catechol–containing fluorescent nanoparticles (green). (*B*) A coating of alginate-catechol on the 10-μm scale. (*C*) A coating of alginate-dopamine on the 100-μm scale. (*D*) A coating of alginate-catechol on the 1-mm scale. (*E–J*) Alginate-catechol gel remains in blood vessels for >4 mo. Immunofluorescence sections show particles inside the hydrogel (pink), cell nuclei (blue), elastin (green, autofluorescence), and red staining for either CD31, a marker for endothelial cells (*E* and *F*), SMA, a marker for smooth muscle cells (*G* and *H*), or MAC-3, a marker for macrophages (*I* and *J*). After 4 mo, the vessel has grown around the hydrogel, and the hydrogel has been covered over by new endothelium and smooth muscle cells and has become incorporated into the blood vessel wall without eliciting the chronic influx of macrophages.

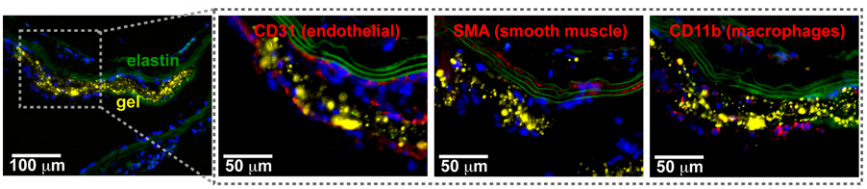

Fig. S5. Carotid arteries coated for 4 d. Immunofluorescence sections show particles inside the gel (yellow), elastin (green autofluorescence), cell nuclei (blue), and red staining for either CD31, a marker of endothelial cells, SMA, a marker of smooth muscle cells, or CD11b, a marker of macrophages.

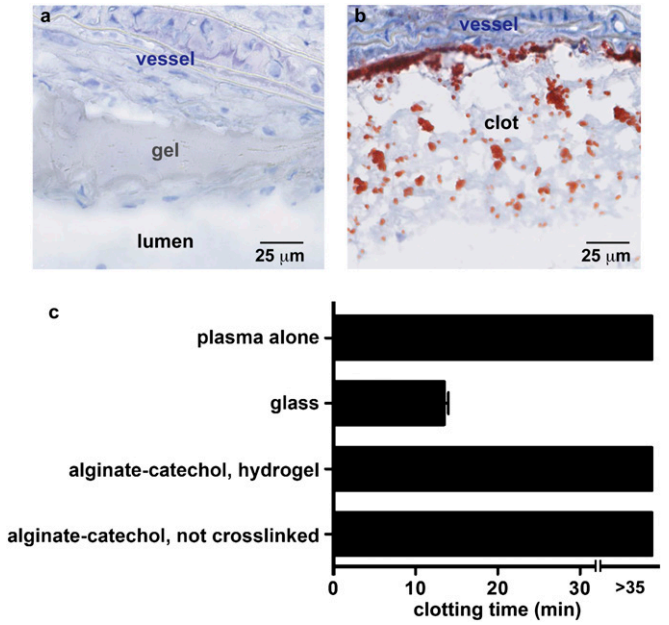

Fig. S6. Alginate-catechol does not initiate blood coagulation in vivo or in vitro. (*A* and *B*) In vivo, histological sections of carotid arteries from WT mice stained for CD41 (brown), a marker of activated platelets. (*A*) Artery coated with alginate-catechol for 30 d. (*B*) Artery without hydrogel that was ligated overnight and formed a blood clot. (*C*) In vitro, clotting time of human blood plasma by alginate-catechol ($n = 4$).

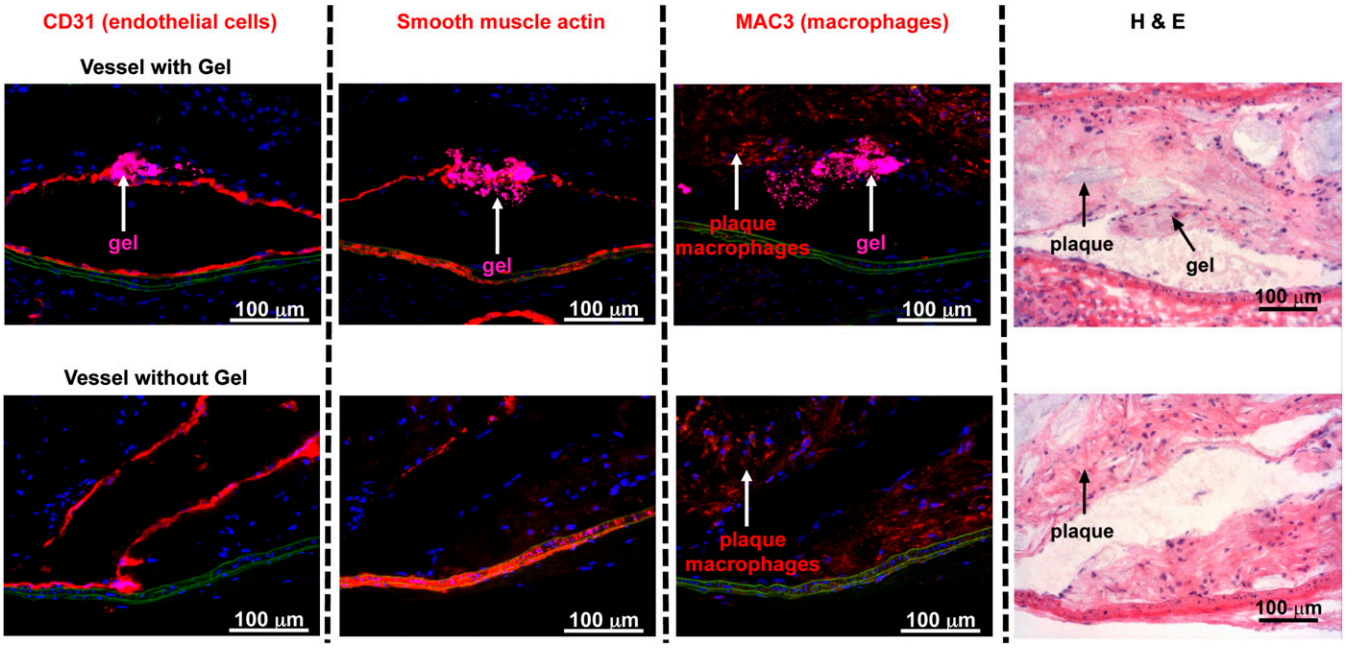

Fig. S7. Adhesion of alginate-catechol (without dexamethasone) to atherosclerotic plaques for 28 d. Without delivery of dexamethasone, macrophages are seen throughout the plaque, similar to the vessel without gel.

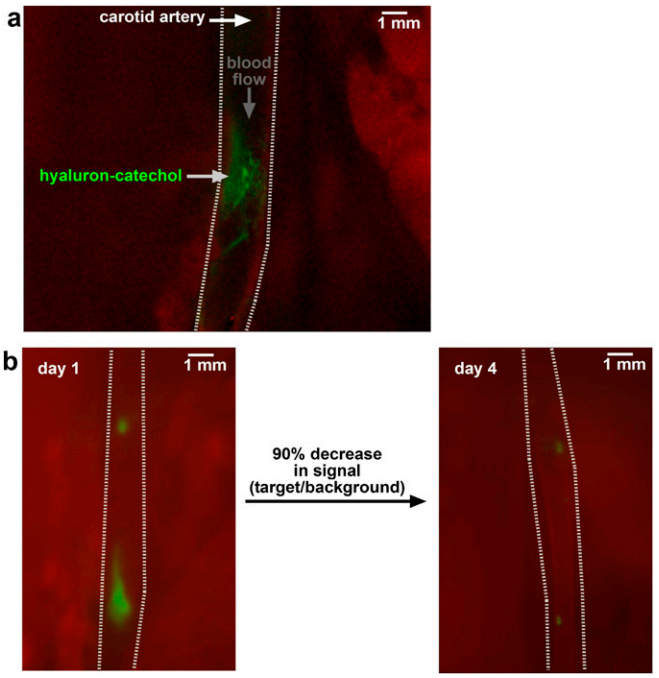

Fig. S8. Hyaluron-catechol can be coated on blood vessels and degrades over time. (*A*) Overlaid fluorescence images from intravital microscopy of hyaluron-catechol containing 0.1-μm fluorescent particles (green) inside of a common carotid artery in a living mouse. Red fluorescence is false-colored autofluorescence from the vessels and surrounding tissue. (*B*) Images showing that the amount of hyaluron-catechol decreased by 90% within 3 d, suggesting that the hydrogel partially degraded while portions of the gel still remained attached to the wall.

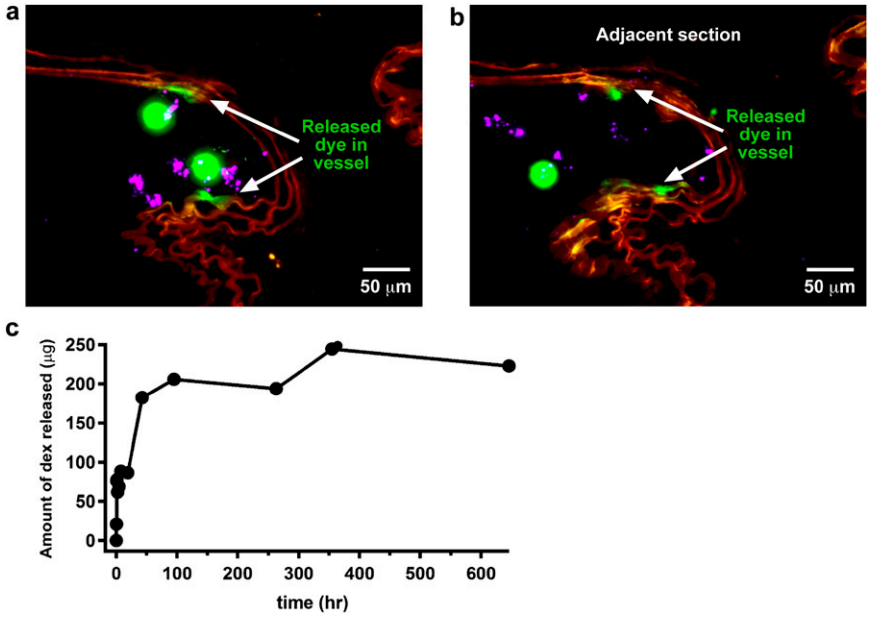

Fig. S9. Release of a fluorescent dye from two PLGA particles into the vessel wall. (*A*) Image from Fig. 3*D* of a histological section showing green fluorescence in the vessel wall near two PLGA particles loaded with BODIPY. Also seen are elastin (red, false-colored autofluorescence) and 0.1-μm fluorescent particles (pink) inside of the gel. (*B*) An adjacent section above the two PLGA particles showing BODIPY is present in the same location of the vessel wall, indicating that the dye entered the wall from the two PLGA particles before when the vessel was sectioned. (*C*) In vitro release profile of dexamethasone from alginate-catechol, measured using an ELISA, complementing Fig. 3*A*.